Time Series Analysis Course

Final project –

Global Temperature

Submitted by:

Diyar Husayyan,214034621 – Technion

Jawad Khatib,214246514 – Technion

Original Data Set : Global Land Temperatures repository

Exogenous Variable: Trends in CO2 - NOAA Global Monitoring Laboratory

Introduction:

Climate change is a defining challenge of our time. To study global warming, we analyse the **Global Land Temperatures dataset**, which provides monthly records from 1900 to 2015. This period aligns with scientific consensus that post-1880 data is more reliable.

Dataset Overview:

- **Date (month and year)**
- **Land Average Temperature (°C)**

After filtering, we verified continuity, standardized the format, and handled any missing values to prepare the series for statistical modelling.

Research Questions:

1. What is the trend in global land temperature since 1900?
2. How does seasonality appear in the series, and has it changed?
3. How well can statistical models forecast future temperatures?
4. Do external variables and change-point detection improve our understanding of the climate signal?

The data:

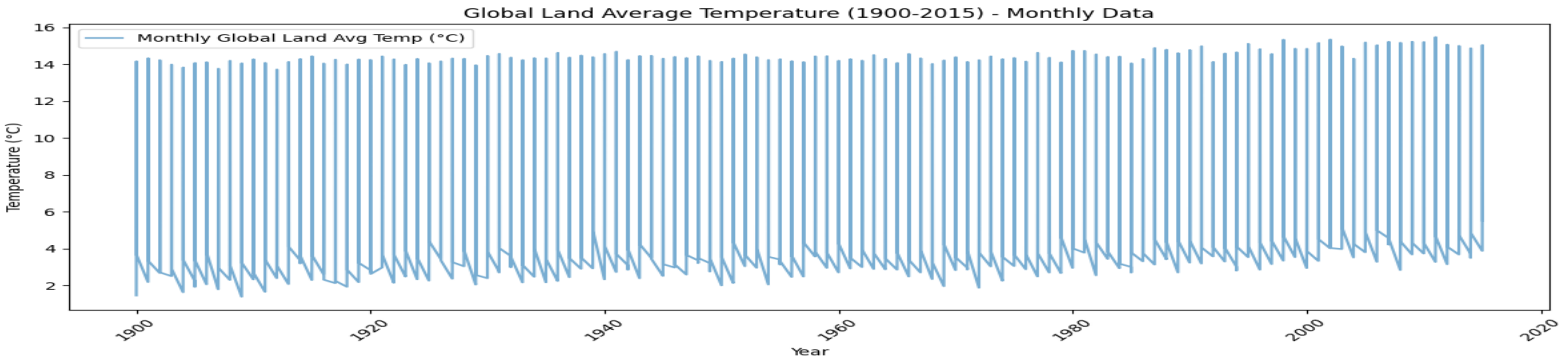

Trend Analysis:

We explored two approaches to estimate the temperature trend:

12-month rolling average: Smooths short-term noise and highlights seasonal effects but masks the long-term upward trend due to its narrow window.

Yearly averaging: Emphasizes the long-term trend more effectively. It clearly shows a consistent increase in global land temperatures, especially after the 1980s.

This comparison highlights that rolling averages are useful for noise reduction, but yearly averages are better suited for visualizing climate trends.

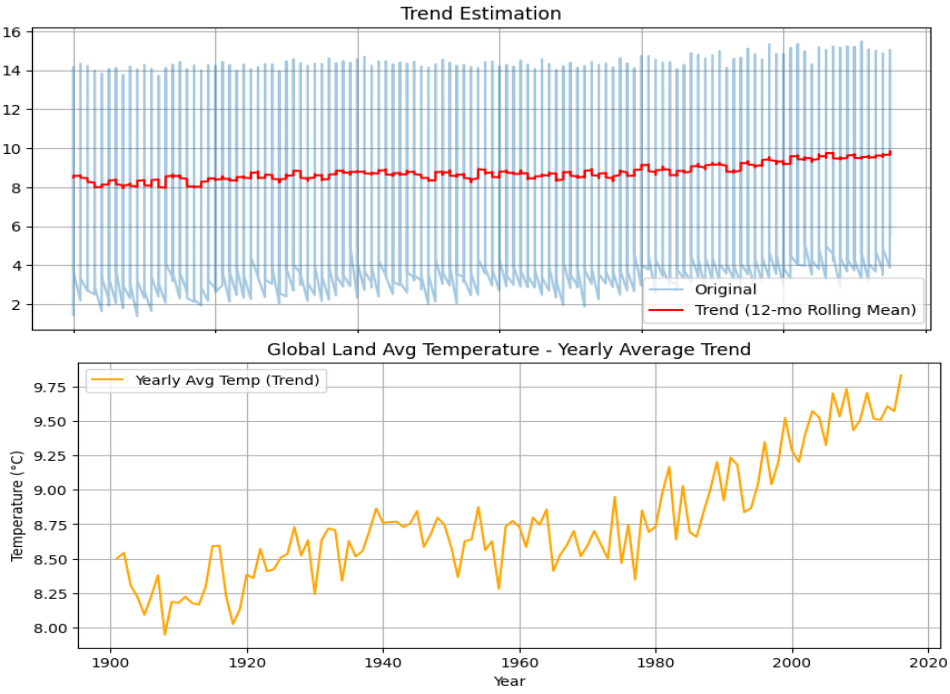

Seasonality Analysis (Manual Estimation):

To estimate the seasonal component, we subtracted the long-term trend and computed the **average deviation for each calendar month** across all years. This reveals a strong and consistent annual temperature cycle:

Peak seasonal effect in **July** (~+5.7°C), **Lowest in January** (~−5.9°C)

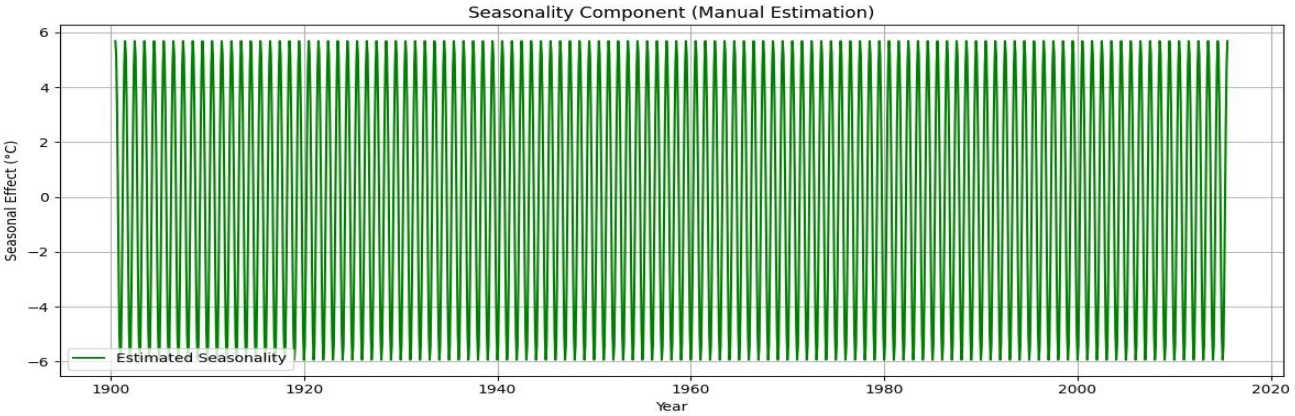

Monthly Seasonal Averages:

1. -5.932
2. -5.427
3. -3.366
4. -0.222
5. 2.633
6. 4.779
7. 5.687
8. 5.197
9. 3.403
10. 0.759
11. -2.545
12. -4.961

To improve readability, we zoomed into the **1955–1980** period:

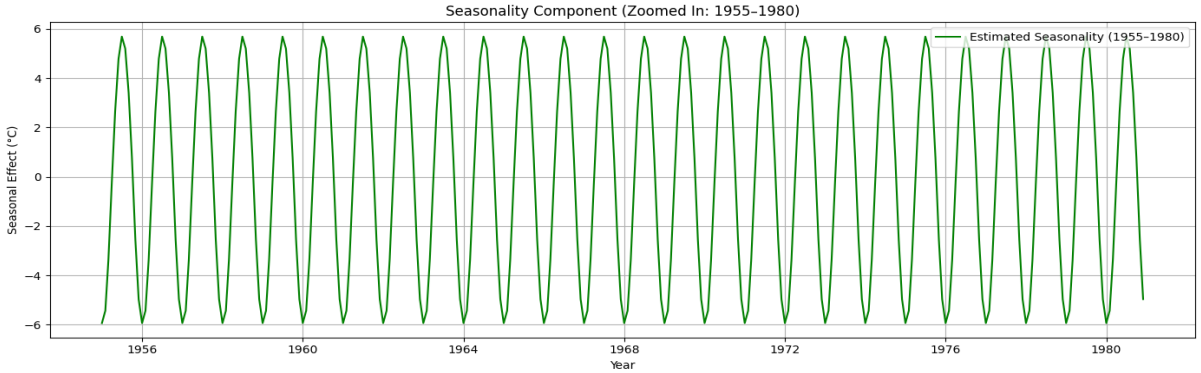

The seasonal wave remains regular and stable, further supporting the presence of strong annual seasonality in global land temperatures.

Residual (Noise) Analysis:

After removing both the trend and the seasonality components from the original time series, the remaining residual (or noise) component captures the irregular and random fluctuations that cannot be explained by systematic patterns

The residual plot shows:

- No clear trend or seasonal pattern
- Fluctuations centred around 0
- Random spikes indicating short-term variability

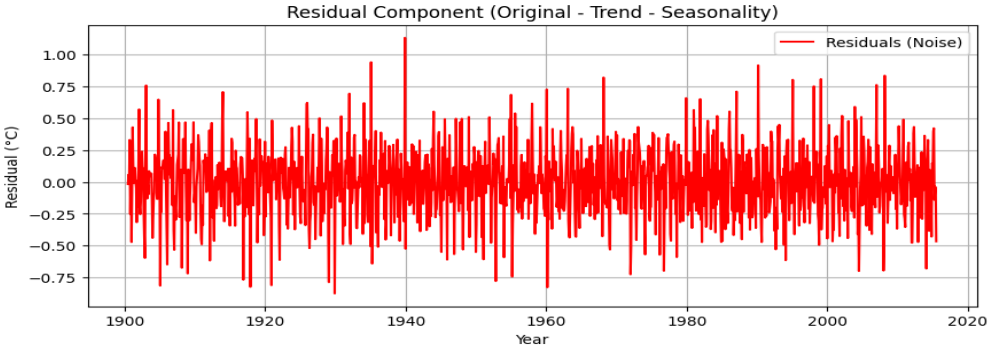

This validates that our manual decomposition was effective, and the residuals can now be tested for stationarity and used for modelling. we applied the Augmented Dickey-Fuller (ADF) test.

The results were as follows:

- **ADF Statistic**: −15.66
- **p-value**: 1.56×10^{-28}

Since the ADF statistic is well below the critical values and the p-value is near zero, we reject the null hypothesis of a unit root. This confirms that the residuals are stationary and suitable for modelling with methods like SARIMA.

Methodologies and Results:

In this section, we apply a series of forecasting models introduced in the course to the processed temperature time series. These models include SARIMA, Prophet, Fourier + Trend Regression.

1. SARIMA

Parameter Justification:

To begin our forecasting analysis, we applied the SARIMA model to the monthly global land temperature series. Based on earlier decomposition of the data, we confirmed the presence of a clear upward trend and a strong seasonal component with a 12-month periodicity. This guided the initial setting of the differencing orders: we used first-order differencing ($d = 1$) to remove the trend and seasonal differencing ($D = 1$) with a period of $s = 12$ to account for the annual cycle.

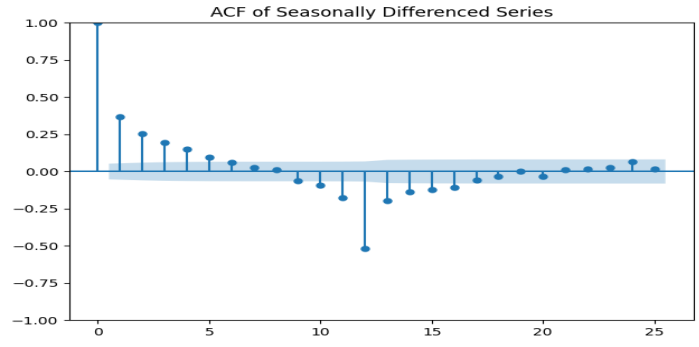

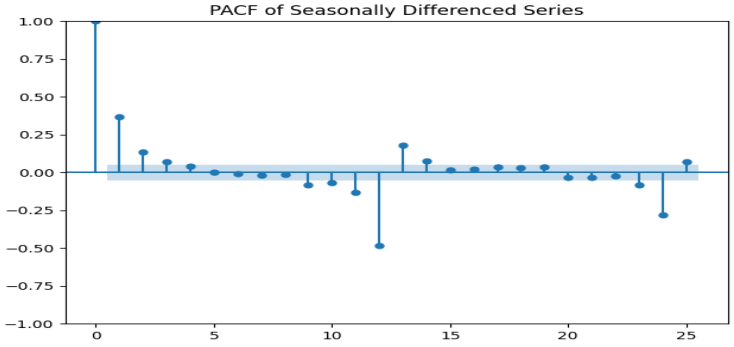

To determine the appropriate autoregressive and moving average parameters, we examined the ACF and PACF plots above of the seasonally differenced series. The ACF plot displayed significant positive correlations at lags 1 to 5 and a seasonal spike at lag 12, suggesting a moving average structure including seasonal MA terms. The PACF plot indicated autoregressive behaviour, with strong spikes at lags 1 to 3 and further significance around lag 12. Based on these insights, we tested five candidate models:

- SARIMA (1,1,1)(1,1,1)[12] SARIMA (2,1,2)(1,1,1)[12] SARIMA (2,1,1)(2,1,1)[12]
- SARIMA (1,1,2)(1,1,2)[12] SARIMA (2,1,0)(2,1,1)[12]

Fitting the Models:
All models were compared using the Bayesian Information Criterion (BIC). The model SARIMA (1,1,2)(1,1,2)[12] yielded the lowest BIC of 580.44, and was selected as the final model.

Residual diagnostics confirmed model adequacy:

- Residuals were centred around zero with no visible trend
- The Q-Q plot and KDE-supported histogram showed near-normality
- The ACF of residuals showed no significant lags — confirming white noise

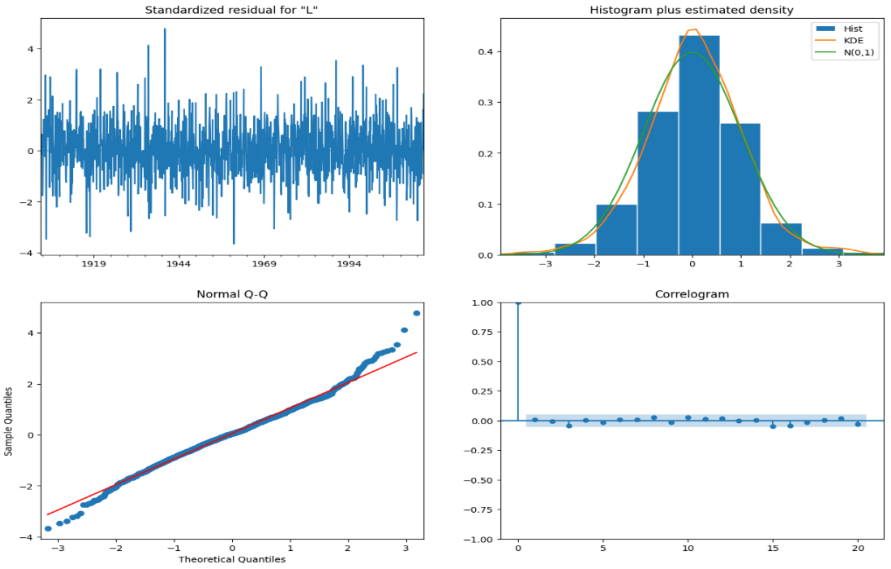

SARIMA (1,1,2)(1,1,2)[12] Forecast Interpretation:

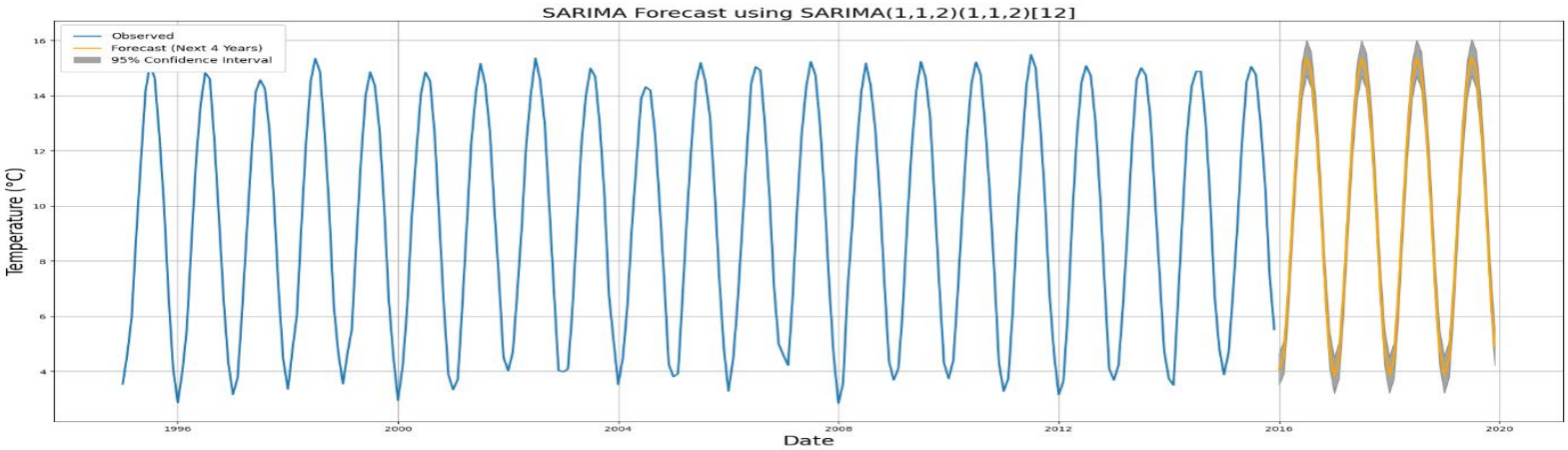

After validating the model, we generated a 4-year forecast beyond 2015, which preserved the seasonal structure and displayed widening confidence intervals over time, as expected. This forecast is shown in the SARIMA prediction plot. The strong fit and robust diagnostics support SARIMA as a valid baseline model for temperature prediction.

2. Fourier + Trend Regression:

We modelled the temperature's periodic component using **Fourier series decomposition** with period T=12 months (annual seasonality). The seasonal signal was reconstructed using the first 6 harmonics of sine and cosine terms

Mathematical Model

The general form of the Fourier model is:

$$\hat{y}_t = \alpha_0 + \sum_{k=1}^{\frac{T}{2}} (\hat{\alpha}_k \cos(\lambda_k t) + \hat{\beta}_k \sin(\lambda_k t)) + \epsilon t$$

Where:

- α_0 is the mean of the series
- λ_k=2πk/T, with T=12 for monthly seasonality
- t is the time index
- ϵt is the residual noise

To incorporate long-term warming, we extended the model with a linear trend term:

$$\hat{y}_t = \alpha_0 + \theta_1 t + \sum_{k=1}^{\frac{T}{2}} (\hat{\alpha}_k \cos(\lambda_k t) + \hat{\beta}_k \sin(\lambda_k t)) + \epsilon t$$

Where:

- α_0 is the mean of the series
- θ_1 represents the trend slope over time

Periodicity Analysis:

To validate the presence of strong seasonal cycles, we used the **periodogram**, a global **F-test**, which strongly rejected the null hypothesis of no periodic structure (F=8585.02>Fcrit=1.80) and **F-tests** for each harmonic to determine statistical significance. The periodogram clearly highlighted a dominant peak at 12 months.

Harmonic k	Period (months)	I_k	F-statistic	Significant?
1	12	24155.59	47160.88	yes
2	6	22.31	43.56	yes
3	4	2.00	3.91	yes
4	3	3.37	6.57	yes
5	2	0.07	0.13	false
6	1	1.31	2.56	false

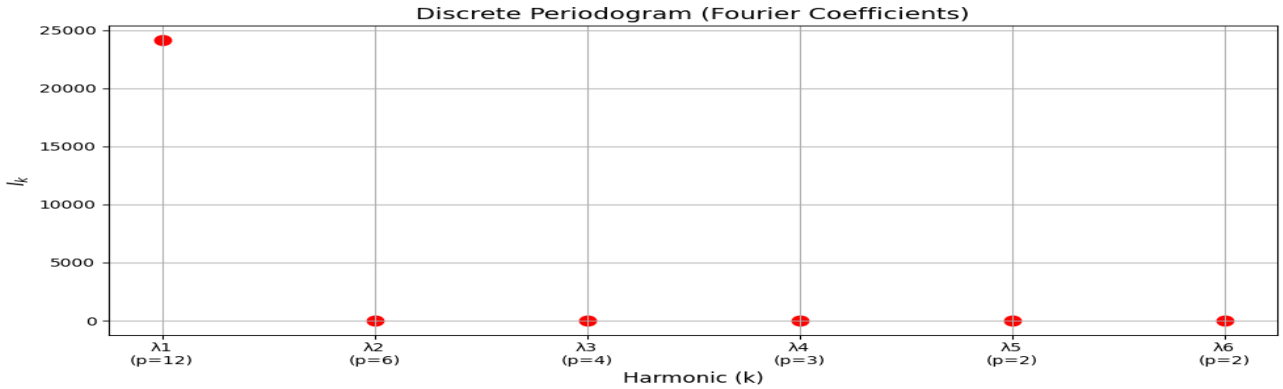

Forecasting with Fourier Models:

We first fit a **Fourier-only** model without a trend. using six harmonics and an intercept. As shown in **plot below**, the model successfully captured the timing of seasonal cycles but **underestimated the peaks** (summer highs) and **overestimated the troughs** (winter lows). This produced a wave with **reduced amplitude**, especially visible in the **forecast period** in **plot below**, where the model consistently predicted lower summer temperatures and deeper winter dips than observed, this happens because the model assumes **fixed amplitude** over time, ignoring changes in temperature range and trend.

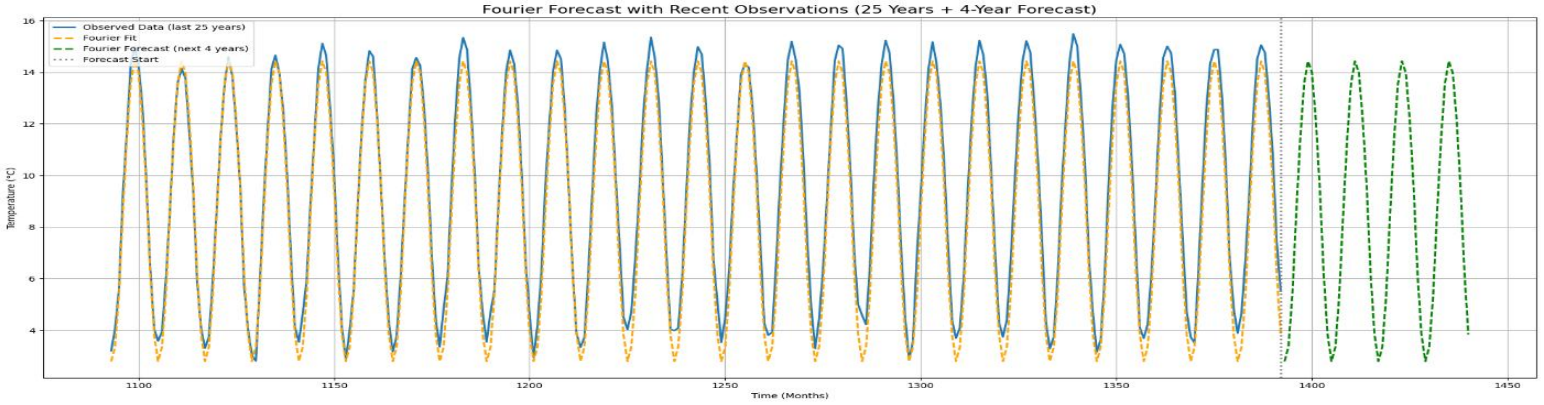

These limitations motivated the addition of a linear time trend in the extended **Fourier + Trend model**:

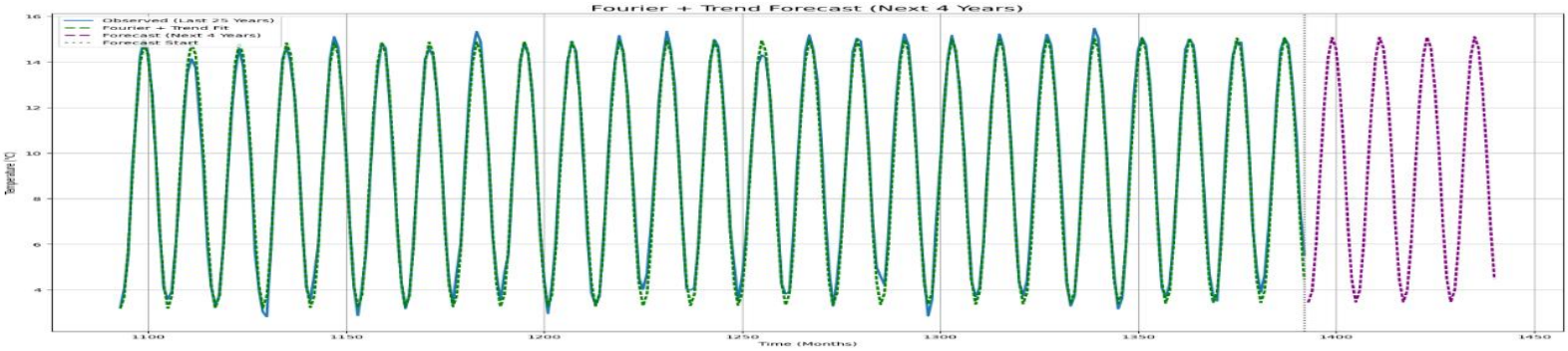

After adding the trend component, the **Fourier + Trend** model achieved better alignment with actual values, and in the forecast region. (blue is the observed, green is Fourier, pink is the forecast)

Residual Diagnostics:

We analysed the residuals of both the **Fourier-only** and **Fourier + Trend** models to assess goodness-of-fit.

For the **Fourier-only model:**

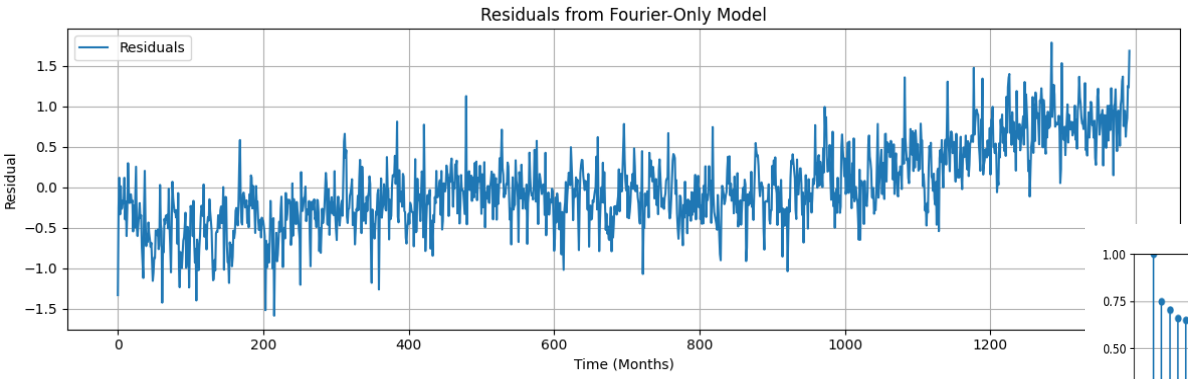

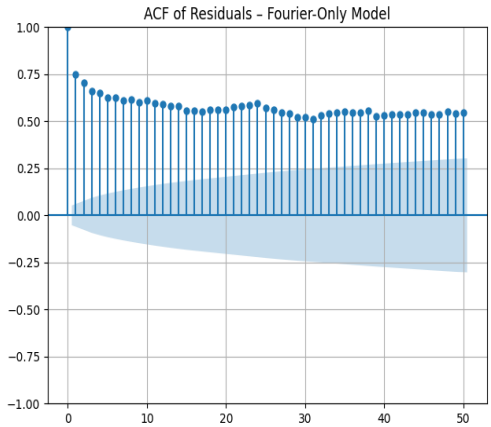

residuals showed clear signs of **non-stationarity** and trend, as seen in the residual time plot and ACF. This confirms that the model failed to capture the long-term warming present in the data**.**

For the **Fourier + Trend model:**

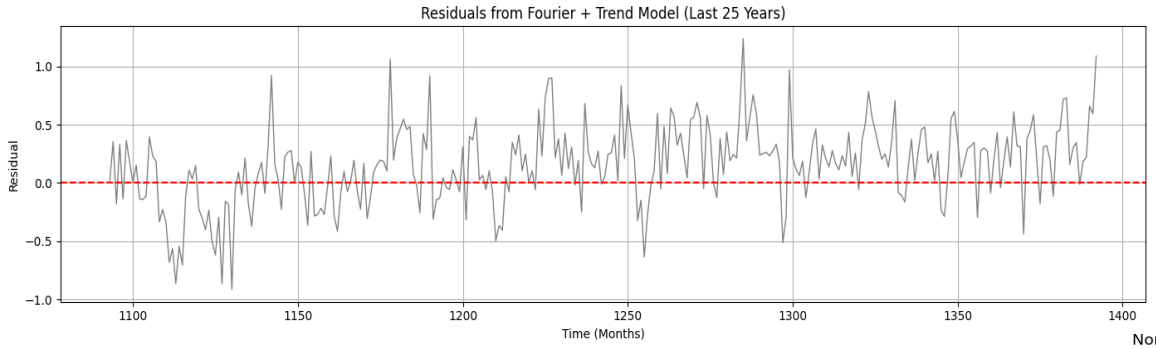

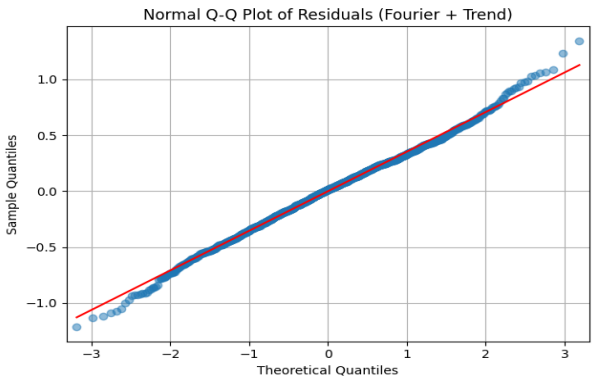

adding the linear time trend significantly improved the residuals. The residuals were centred around zero, with no clear temporal pattern. The Q-Q plot showed approximate normality, and the residual histogram supported this.

However, the ACF plot still revealed significant autocorrelation at all lags. This suggests that while the model captures trend and seasonality well, it does not model stochastic dependence — a limitation of deterministic models like Fourier regression. This reinforces the need for models like SARIMA, which explicitly address temporal correlation.

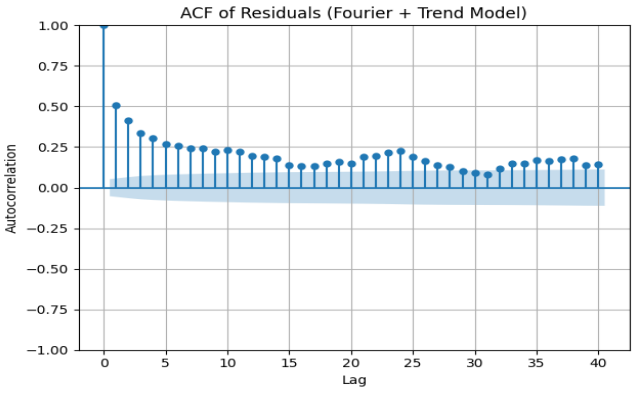

3. Prophet model:

We selected Prophet because it is well-suited for capturing complex time series behaviours, including nonlinear trends and various seasonal effects. Its additive framework automatically incorporates multiple seasonality's—such as yearly, weekly, and daily patterns—and can also account for holiday impacts when needed. For our dataset, yearly seasonality is most critical, and Prophet's flexibility (through adjustable parameters for seasonality and trend strength) enables robust forecasting with relatively narrow uncertainty intervals.

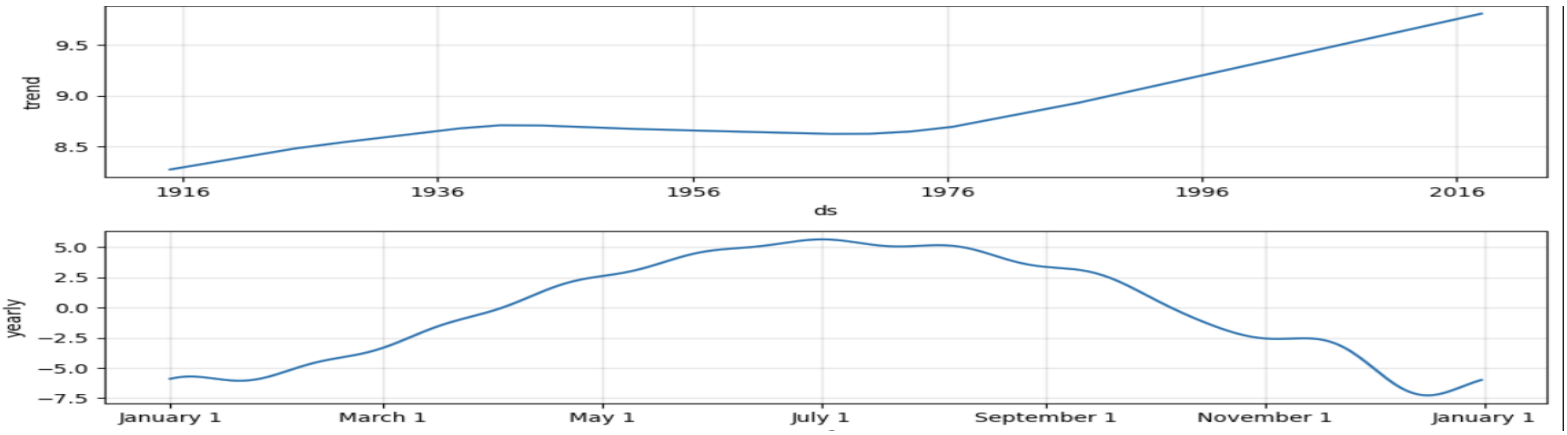

In the top panel, we observe the trend component, which spans from the early 1900s to 2020. The slope of this line indicates a gradual warming trend over the decades, reflecting a rise in global land temperatures. In the lower panel, we see the yearly seasonal pattern, which peaks around mid-year (higher temperatures in the summer months) and dips around the start of the year.

Prophet Forecast:

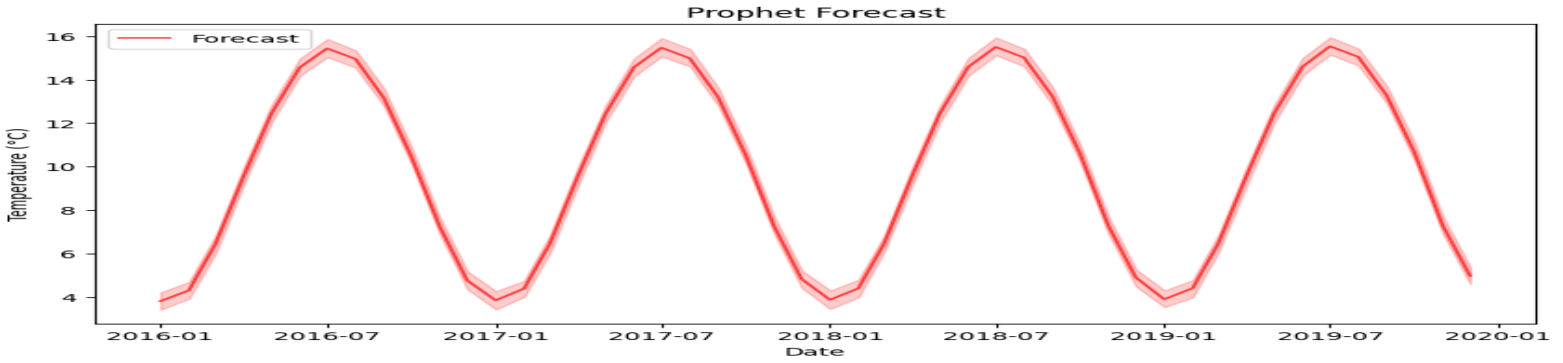

Here, we highlight a short-term forecast where the red line represents predicted monthly temperatures, and the red shading denotes the model's confidence interval. The clear wave-like pattern indicates Prophet's ability to capture the pronounced annual highs and lows. The relatively narrow band around the forecast suggests moderate certainty in these short-term predictions.

Prophet Full:

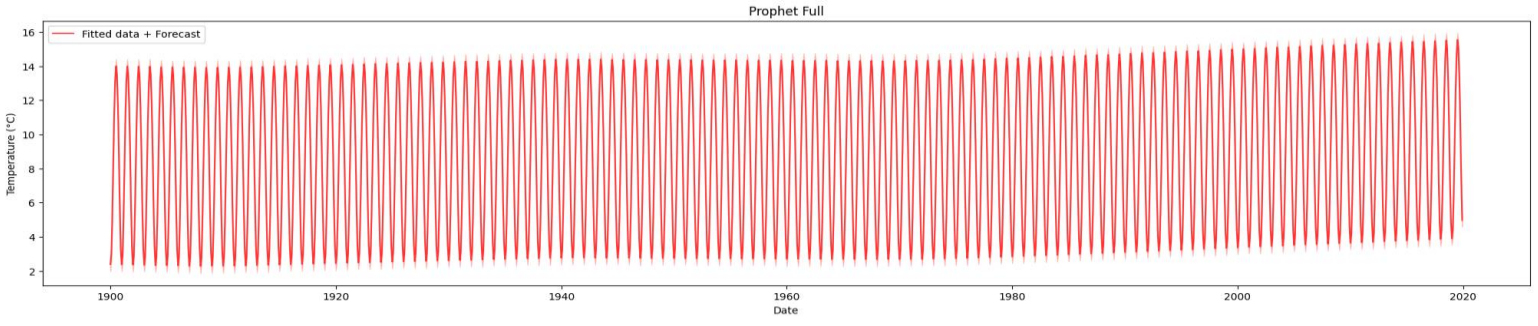

For better plot:

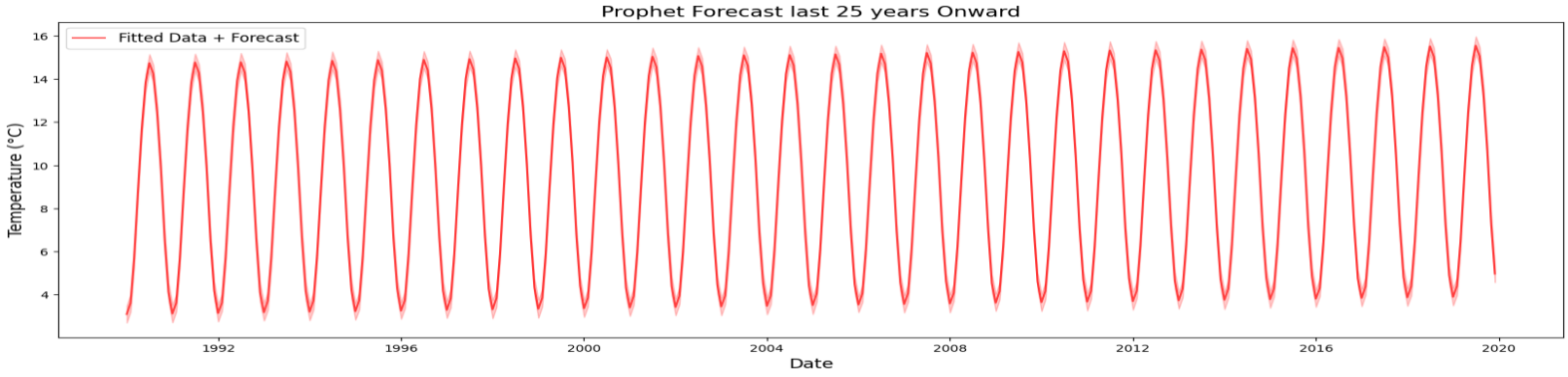

Finally, this figure shows the entire fitted dataset plus the extended forecast from the earliest available date up to around 2020. Each year's seasonal fluctuation is visible, and the gentle upward slope reflects the long-term warming trend. For improved clarity, we also display the forecast in the last 25 years with the additional 4 years forecast, providing a more focused view of recent trends and how the model extends them into the near future.

Model Comparisons:

To assess forecasting accuracy, we trained each model on data up to **December 2010**, then predicted the next five years (**2011–2015**). Forecasts were evaluated using **MSE**, **MAE**, and **RMSE**.

As shown in **Table** , the **SARIMA(1,1,2)(1,1,2)[12]** model outperformed others with the lowest error across all metrics (MSE = 0.0873, RMSE = 0.2955), effectively capturing both seasonality and autocorrelation.

The **Prophet model** delivered comparable performance (RMSE = 0.3023), benefiting from flexible seasonal and trend components. Its forecasts aligned well with the annual cycle, as seen in **Figure down**.

The **Fourier + Trend model**, while accurate in structure, produced higher errors due to its deterministic nature. It failed to capture stochastic dependencies, leading to **residual autocorrelation** and larger forecast deviations.

These results confirm that **SARIMA** is the most reliable model for this dataset, though Prophet remains a strong alternative with simpler tuning and good generalization

index	MSE	MAE	RMSE
SARIMA	0.0873	0.2187	0.2955
Fourier + Trend	0.1687	0.349	0.4107
Prophet	0.0914	0.2314	0.3023

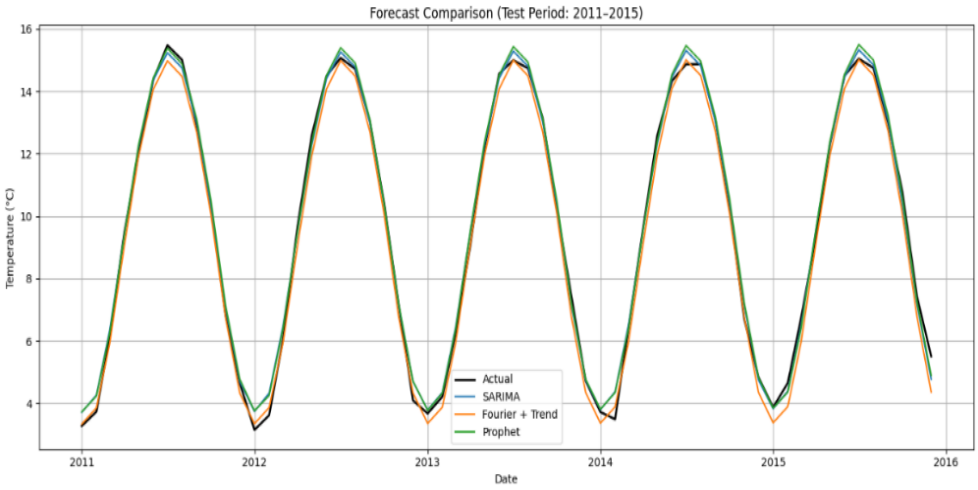

Part 3: Modelling with Exogenous Variables:

In this part, we investigated the effect of including an exogenous variable — the atmospheric CO_2 trend — on the modelling of global land average temperature. The goal was to assess whether incorporating this external factor, which is conceptually linked to global warming, improves model performance in predicting temperature over time.

Feature Construction:

To capture both seasonal and long-term patterns in the temperature series, we constructed a set of features including:

- A linear time trend to capture global warming
- Fourier terms with K=6 harmonics to capture annual and sub-annual seasonality
- An exogenous variable: the CO_2 trend, representing the atmospheric concentration of carbon dioxide over time

The feature matrix X thus included an intercept, the time index t, 12 Fourier components (sine and cosine), and the CO_2 trend. The response variable y was the monthly land average temperature from 1979 to 2015. The data was split into 80% training and 20% test sets.

Models and Evaluation:

We trained several models using the constructed features: Linear Regression, Ridge, Lasso, Support Vector Regression (SVR), Decision Tree, Random Forest, and XGBoost. Each model was evaluated using the Mean Squared Error (MSE) on the test set.

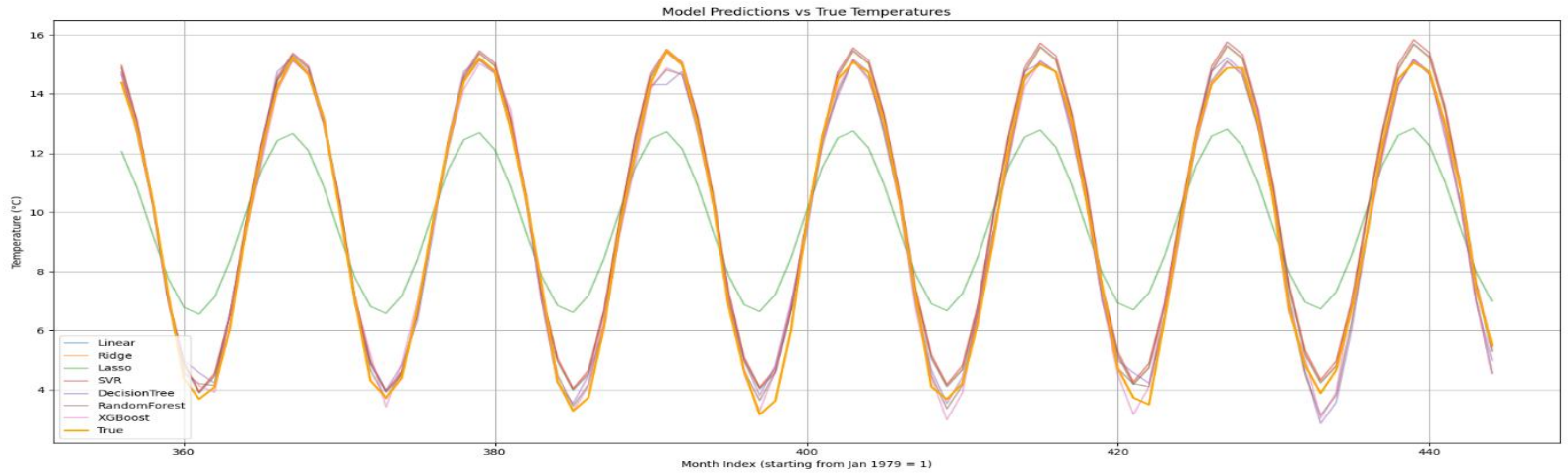

Among all models, Random Forest achieved the lowest MSE of 0.103, followed by XGBoost and Linear Regression. The performance across models was relatively close, except for Lasso, which significantly underperformed due to over-penalization and likely multicollinearity.

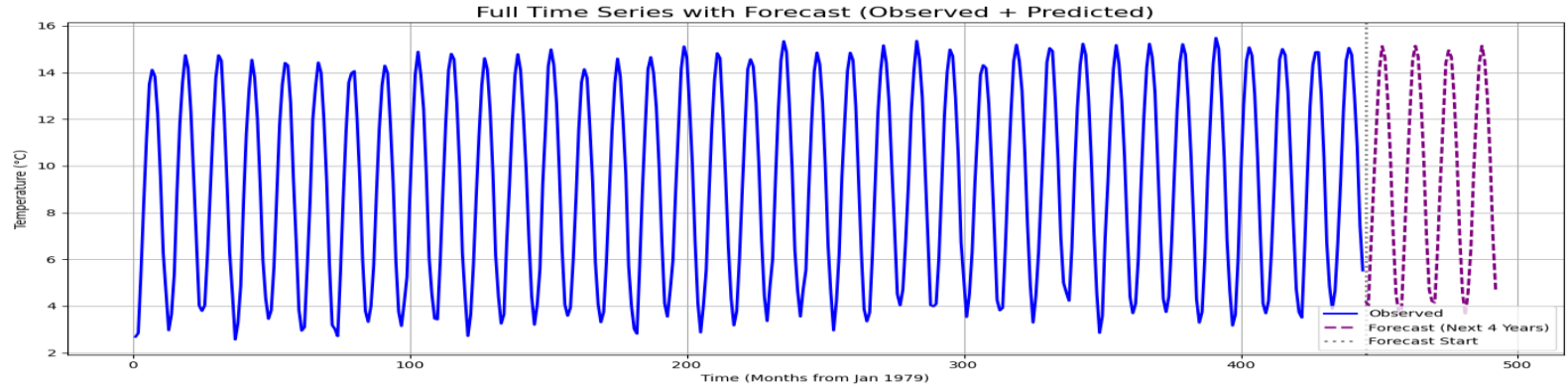

To further evaluate the impact of the CO_2 trend, we retrained the Linear Regression model without it. Interestingly, the MSE dropped from 0.1753 (with trend) to 0.0855 (without trend), and the MAE dropped from 0.3384 to 0.2198. The BIC also improved (from −83.15 to −151.56), indicating that the CO_2 trend not only failed to enhance predictive performance but also added unnecessary complexity.

Residual diagnostics confirmed these findings. While the linear model without CO_2 showed a slight worsening in autocorrelation at two lags, overall residual behaviour remained similar. In contrast, the Random Forest model showed a minor MAE improvement after removing the CO_2 trend (from 0.2394 to 0.2361), though MSE slightly increased. This suggests that while Random Forest can leverage some nonlinear signal, the CO_2 trend was not a meaningful predictor. Its residuals appeared closer to white noise, highlighting that more flexible models are better suited to capturing subtle patterns in temperature dynamics.

Residual Diagnostics:

To evaluate the quality of the Random Forest model, we analysed its residuals using several standard diagnostic tools. The residuals were computed as the difference between the actual temperature values and the model's predictions on the test set.

The residuals over time showed no visible trend or seasonal pattern and were centred around zero. The mean of residuals was approximately 0.038, indicating no systematic bias in the predictions.

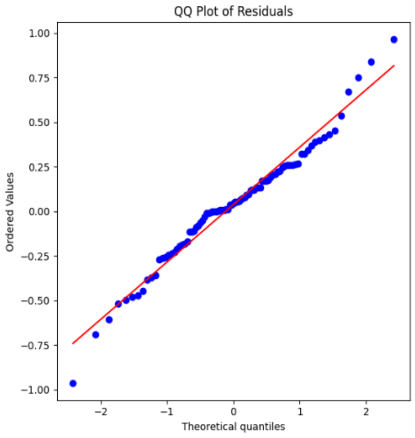

The histogram of residuals appeared approximately symmetric and bell-shaped, suggesting the errors were normally distributed. The QQ plot further supported this, with residuals closely following the expected normal quantiles.

Most importantly, the ACF plot of residuals showed no significant autocorrelation across 24 lags. This suggests that the Random Forest model successfully captured the time-dependent structure in the data, leaving behind residuals that resemble white noise. This is a strong indication of a well-fit model.

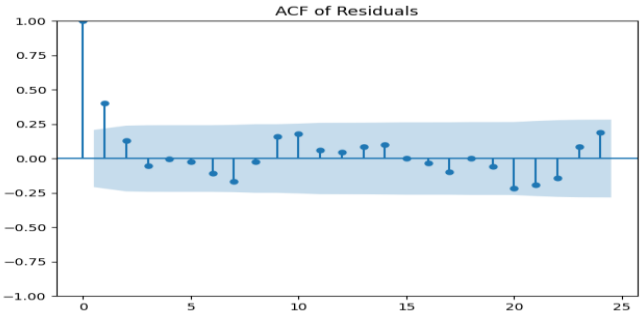

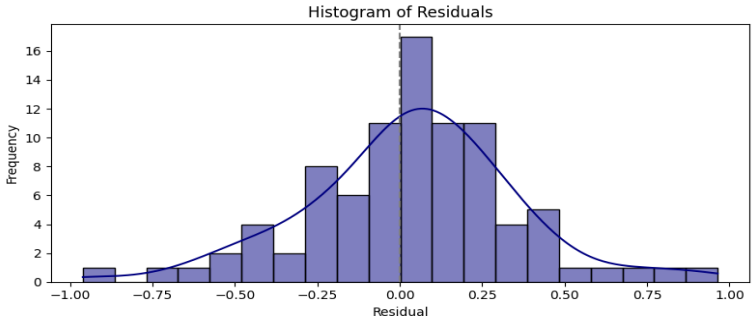

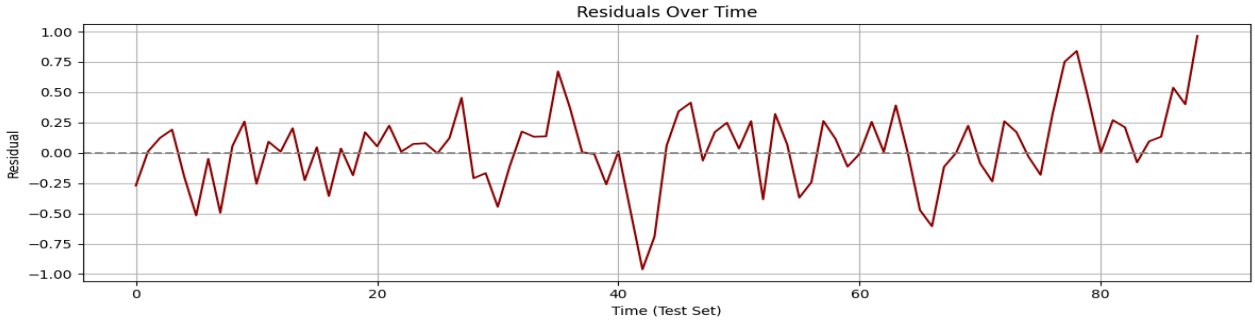

Correlation Analysis:

To assess the explanatory power of the CO_2 trend, we computed the Pearson correlation between the CO_2 trend and global land average temperature across the study period (1979–2015). The resulting correlation was only 0.076, indicating a very weak linear relationship between the two variables.

This was further confirmed by a scatter plot of CO_2 trend vs. temperature, which showed no clear upward or downward pattern. The lack of strong linear correlation explains why the inclusion of the CO_2 trend did not improve the performance of the Linear Regression model, and in fact slightly worsened it. However, nonlinear models like Random Forest may still leverage the CO_2 signal through more complex interactions.

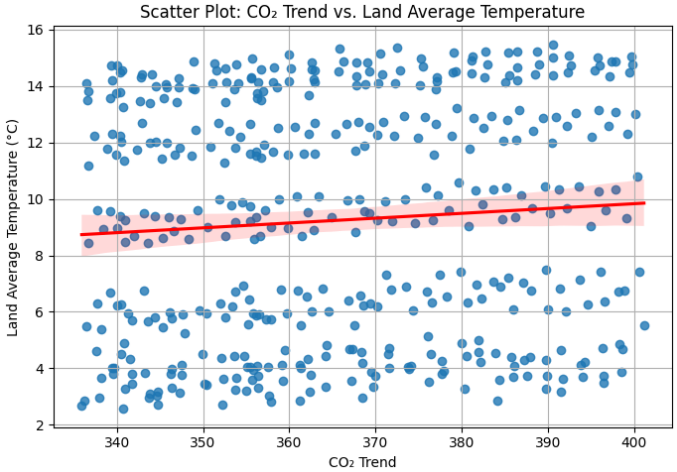

Part 4: Change-Point Detection

In this section, we focused on identifying **structural changes** (change-points) in global land temperatures using **CUSUM-based methods**. The analysis was performed on the **residual component** after removing trend and seasonality from the original time series.

1.Residual Calculation:
We began by decomposing the original series into trend, seasonality, and residuals using the model from earlier parts.

2.ACF Analysis

Before applying change-point detection, we conducted **autocorrelation checks** on the residuals:

- First, we plotted the **ACF of the full residual series**, which showed a few minor spikes.
- Then we split the residuals into **12 monthly series** and computed the ACF for each month individually.
- For **every month**, all lags were found to be **within the confidence interval**, indicating that the residuals were sufficiently white (uncorrelated) for applying CUSUM.

This justified treating each monthly residual series as approximately independent over time.

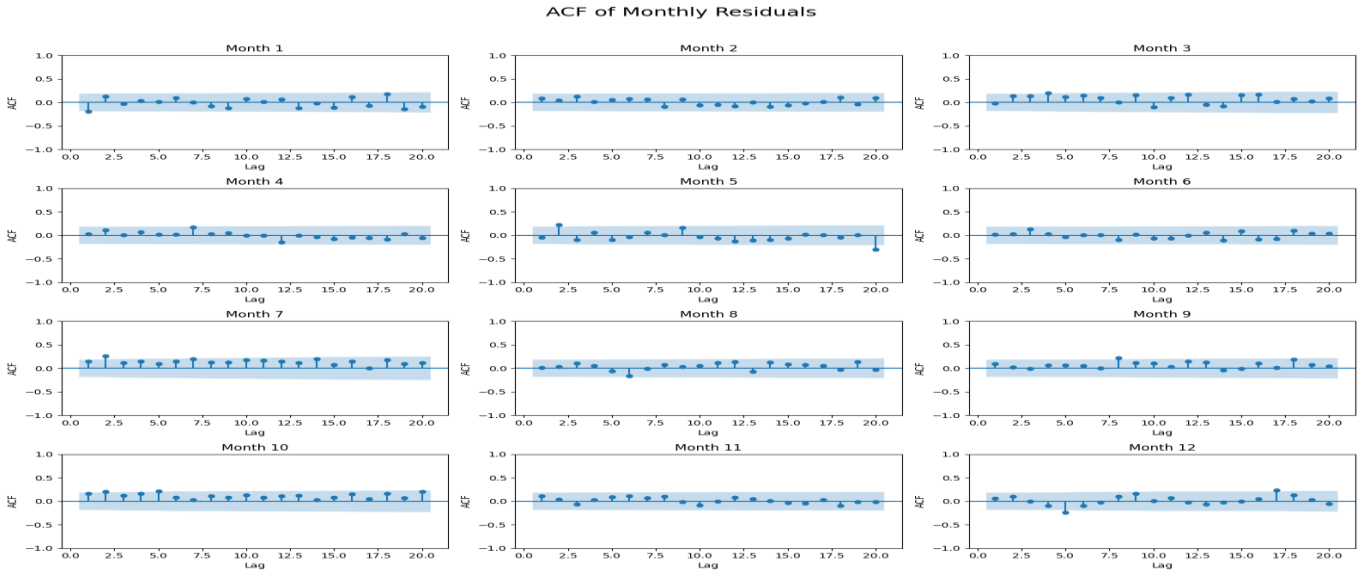

3.Monthly Decomposition:
To account for seasonality more precisely, we split the residual series into 12 monthly time series, one for each calendar month (e.g., all Januarys across years, etc.).

This allowed us to detect **month-wise shifts** in the distribution of residuals, avoiding artificial detection due to seasonal structure.

4.Customized CUSUM Parameters:
For each monthly series, we applied the **CUSUM algorithm**, using customized parameters per month based on its standard deviation (σ):

- **Drift k =** $\frac{\Delta}{2}$ where **Δ = 0.4σ**
- **Threshold h = log B = 5σ**

This dynamic tuning allowed us to control for different variabilities in each month.

Each detected change-point was associated with a year, and a **score** was maintained for how many months had change-points in each year.

5.Visualization:

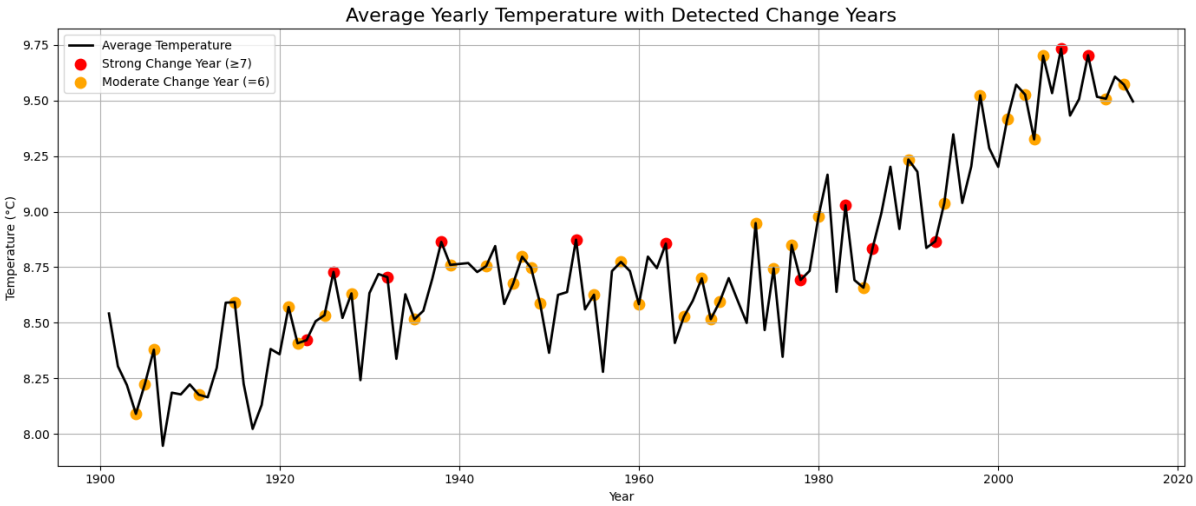

We plotted the average yearly temperatures and marked change years:

- **Red dots** for strong change years (≥ 7 months)
- **Orange dots** for moderate change years (= 6 months)

This helps visually validate that change years are associated with increasing and decreasing temperatures.

Conclusion:

This project analysed global land temperature trends using monthly data from 1900 to 2015. After decomposing the series into trend, seasonality, and residuals, we confirmed a long-term warming trend and a strong, consistent seasonal cycle.

We tested multiple forecasting approaches:

- **SARIMA(1,1,2)(1,1,2)[12]** emerged as the best model, capturing both seasonality and autocorrelation, with the lowest forecast errors.
- **Prophet** performed similarly, leveraging flexible trend and seasonal components, and offered strong out-of-the-box accuracy.
- **Fourier + Trend Regression** captured deterministic structures well but suffered from residual autocorrelation, leading to weaker forecasts.

In Part 3, we introduced **exogenous CO_2 trend data**. While it slightly **improved the performance of Random Forest**, the effect was not significant. In contrast, **linear regression** showed **no improvement** with the addition of CO_2 — in fact, the performance slightly worsened, which aligns with the weak correlation (~0.07) between CO_2 and temperature.

Finally, change-point detection on the residuals using **CUSUM** revealed key structural shifts in the climate system, flagging years such as 1986, 1978, 1932, and 1993 — aligning with historical changes in global temperature behaviour.

In summary, **SARIMA provided the most robust forecasting performance**, while Prophet proved highly usable with minimal tuning. Fourier models offered interpretability but lacked stochastic modelling. Machine learning showed potential when combined with Fourier features, though exogenous CO_2 did not add significant predictive value. These findings emphasize the value of hybrid approaches and residual diagnostics in climate time series analysis.